IOPscience iopscience.iop.org

Home Search Collections Journals About Contact us My IOPscience

Excimer laser and rapid thermal annealing stimulation of solid-phase nucleation and crystallization in amorphous silicon films on glass substrates

This article has been downloaded from IOPscience. Please scroll down to see the full text article.

1996 J. Phys.: Condens. Matter 8 273

(http://iopscience.iop.org/0953-8984/8/3/007)

View the table of contents for this issue, or go to the journal homepage for more

Download details:
IP Address: 171.66.16.179
The article was downloaded on 13/05/2010 at 13:08

Please note that terms and conditions apply.

J. Phys.: Condens. Matter **8** (1996) 273–286. Printed in the UK

Excimer laser and rapid thermal annealing stimulation of solid-phase nucleation and crystallization in amorphous silicon films on glass substrates

M D Efremov†, V V Bolotov‡, V A Volodin†, L I Fedina† and E A Lipatnikov†

† Institute of Semiconductor Physics, Siberian Branch of Russian Academy of Sciences, pr. ak. Lavrentjeva 13, Novosibirsk 630090, Russia
‡ Institute of Sensor Microelectronics, Siberian Branch of Russian Academy of Sciences, pr. Mira 55a, Omsk 644077, Russia

Received 19 June 1995, in final form 27 September 1995

Abstract. The solid-phase crystallization process in thin amorphous silicon films on glass substrates was studied with application of excimer laser annealing (ELA) and rapid thermal annealing (RTA) for stimulation of nucleation. Use of ELA allowed us to create homogeneous polycrystalline silicon films on glass with grain sizes up to 3 μm at temperatures below 550 °C. Use of RTA reduced the incubation time of nucleation from 100 to 6 h. The textured silicon films on glass with predominant orientation (110) and sizes of textured areas up to 30 μm were manufactured using excimer laser stimulation of nucleation. The influence of the mechanical stress mechanism on grain orientation was suggested, and it was theoretically shown that internal stresses retard the nucleation process. The addition of deformation to the chemical potential difference was estimated for nucleation in amorphous silicon as 11.4 meV per nucleated atom.

1. Introduction

Research in the field of crystallization of silicon thin films on glass substrates has attracted much attention in recent years. This research was aimed at the creation of uniform polycrystalline silicon (poly-Si) films with a high carrier mobility to improve the characteristics of thin film transistors (TFTs). TFTs have broad application in active matrix liquid-crystal displays (AMLCDs), in sensor devices and in other branches of electronics. The wide perspectives of AMLCD applications have stimulated scientific investigations based on the theory of nucleation and crystallization [1–6].

One of the main problems in TFT manufacturing is the low strain-point temperature of the low-cost glass substrates. For example, the widely used glass Corning 7059 has a strain-point temperature of 593 °C. The conventional methods CVD and LPCVD work at temperatures above 620 °C [7] and, therefore, are not suitable for TFT production. Many efforts have been applied to develop low-temperature technology (at least, below 550 °C) for the creation of poly-Si films on glass structures. For example, the poly-Si films grown by the plasma chemical vapour deposition (PCVD) technique at temperatures lower than the strain-point temperature of Corning 7059 (300–450 °C [8, 9]) have a columnar small-grain-size structure [8–10] and consequently a low field-effect mobility. Another technique for manufacturing thin poly-Si films is based on the crystallization of amorphous silicon

0953-8984/96/030273+14$19.50 © 1996 IOP Publishing Ltd

(a-Si) films deposited by PCVD or PECVD at low temperatures (200–300 °C). The low-temperature solid-phase crystallization (SPC) of a-Si films during long-time isothermal annealing (up to 150 h) leads to formation of polycrystalline films with relatively large grain size (maximum about 3 μm); the grains, however, have a dendritic form and a wide dispersion of sizes with prevalence of grains with small sizes [10, 11]. The carrier mobility was observed to be relatively small in these films. Rapid thermal annealing (RTA) at higher temperatures with a low thermal budget (in order to avoid overheating of the substrate) has also been widely used [12, 13]. In this case, poly-Si films also have a small-grain-size structure with very wide dispersion of grain sizes. Amongst various methods of manufacturing of the poly-Si films on glass, nanosecond excimer laser crystallization seems to be the most promising [14–18]. Usually, this method is applied for liquid-phase crystallization (LPC). The typical grain size in poly-Si films manufactured with the use of excimer laser LPC is less than 0.1–0.2 μm. There is also the problem of non-uniformity of the films in laser beam overlap regions.

In our study we have mainly investigated the problems of the SPC of a-Si films on glass substrates. Excimer laser annealing (ELA) and RTA were applied to stimulate the formation of stable nuclei of crystalline phase in amorphous media [19, 20]. This approach is an important new technique in the technology of manufacturing poly-Si films on glass. Introduction of a low concentration of nuclei by the use of ELA and RTA was applied to increase the grain sizes. A low concentration of initial nuclei in as-deposited amorphous films was established ([10], and references therein) to provide beneficial conditions for enlarging the grains, because the adjacent grains grow until they impinge on each other. The use of ELA and RTA makes it possible to introduce nuclei which grow during the subsequent thermal annealing, while the spontaneous homogeneous and heterogeneous critical nuclei have not yet appeared. In this way, the final concentration and the size distribution of crystallites were expected to be determined by the concentration of nuclei injected by the ELA and RTA treatments. To increase the crystallite sizes it is sufficient to decrease the concentration of nuclei introduced.

2. Experimental details

The structures used in the experiment were processed as follows. The a-Si films with a thickness of 1000 Å were deposited on previously annealed Corning 7059 substrates using PCVD at 230 °C. Both doped and undoped a-Si films were used in the experiment. Doping was carried out by ion implantation of phosphorus with a dose of 2×10^{13} cm^{-2}. The properties of the a-Si films were analysed using Raman spectroscopy, infrared (IR) spectroscopy, electron spectroscopy of characteristic radiation, and measurements of conductivity versus temperature.

The treatments given in table 1 were used in the experiments.

Table 1. Treatments used in the experiments.

Treatment	Parameters and conditions
Isochronous annealing (IA)	30 min; 200–500 °C; step, 50 °C; N_2
Isothermal annealing (TA)	30 min–120 h; 550 °C; N_2
RTA	1 s–15 min; 600–900 °C; N_2
ELA	5 ns pulse; 75–300 mJ cm^{-2}

Processed structures were investigated using Raman spectroscopy, measurements of conductivity versus temperature, transmission electron microscopy (TEM) and high-resolution electron microscopy (HREM). Raman spectra were taken with the use of a double spectrometer equipped with a cooled photomultiplier and photon-counting electronics. The spectra were acquired in the back-scattering geometry at room temperature in the optical phonon region. The parameters of the peaks related to the Raman scattering of photons by optical photons (the amplitude, the position and the width) were determined from best-fit Gaussian lineshapes. In a-Si, phonons with various wavevectors can participate in Raman scattering. The Raman spectrum of a-Si includes a broad peak at around 480 cm^{-1} corresponding to scattering in transverse optical (TO) phonon modes. The form of this peak can give information about the structure of a-Si and, from these data, one can determine the bond angle deviation $\Delta\theta$, which characterizes the stability of the a-Si structure [21–23]. The width Γ of the TO phonon line is determined by the following expression:

$$\Gamma = 15 + 6\Delta\theta$$

where Γ and $\Delta\theta$ are in reciprocal centimetres and in degrees, respectively.

In microcrystalline Si the position of the Raman peak is within the range from 500 to 520 cm^{-1}, depending on the dimensions of the crystallites, if their dimensions are less than 500 Å [24, 25]. Dispersion of the crystallite dimensions causes broadening of the Raman peak. When the microcrystallite sizes are larger than 500 Å, then the position of the Raman scattering peak is nearly the same as that of single-crystal Si [24, 25]. The amplitude of this peak depends on the crystallinity of the film. From Raman spectroscopy data, one can analyse the phase composition of the films using the method described elsewhere [26–28]:

$$a = I_c/(I_c + I_a\Sigma_c/\Sigma_a)$$

where a is the crystal part of the film, I_c and I_a are the integrated intensities of the crystalline and amorphous peaks, respectively, and Σ_c and Σ_a are the cross sections of the Raman scattering for the crystalline and amorphous phases, respectively. The value of the ratio Σ_c/Σ_a has been reported to vary from about 0.1 to 0.88 [27]. A ratio of 0.88 is widely used for microcrystalline Si and it was used in our work.

Direct information about the size of grains, their size dispersion and the amount of defects in the films was obtained from the electron microscopy data. TEM analysis was carried out after separation of the silicon films from the glass substrates using etching in HF acid and subsequent deposition of these films onto copper net.

The conductivity of films with deposited Al contacts was measured in the temperature region from 0 to 250 °C in order to determine the activation energy of conductivity. Absorbance spectroscopy, taking into account light interference, enabled us to obtain the refraction index and the optical band gap of the films.

3. Experimental results

3.1. Properties of a-Si films

A broad peak (typical of an amorphous phase without microcrystallites) was observed in the Raman spectra of initial a-Si (figure 1, curve 1). The calculated bond angle deviation $\Delta\theta$ was estimated to be about 7.5°, which corresponds to the stable structure of a-Si [21]. Thermal annealing of these films in the temperature range 200–350 °C leads to an increase in the intensity of the Raman scattering on TO phonons (figure 1, curves 2 and 3) without essential changes in bond angle deviation. The estimated (from the IR data) concentration

of hydrogen was about 20 at.%. The analysis of the IR absorption spectrum as well as of the Raman spectrum (figure 2) enabled us to conclude that the hydrogen in a-Si films was bonded in two states: Si–H (2000 cm^{-1}) and $Si–H_2$ (2090 cm^{-1}) with a prevalence of Si–H states. The optical band gap was determined to be about 1.85 eV. The value of the band gap corresponded well to the high concentration of hydrogen in the films. The conductivity of the a-Si films was $1.36 \times 10^{-9}\ \Omega^{-1}\ cm^{-1}$ (at a temperature of 300 K) with an activation energy of 0.78 eV (figure 3). These films also had a high photoconductivity. The values presented are usual for a-Si with a high concentration of hydrogen and low concentration of recombination centres.

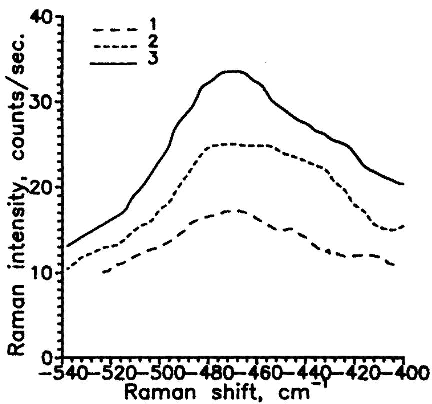

Figure 1. Raman spectra of a-Si films on glass after thermal annealing: curve 1, initial film; curve 2, $T =$ 200 °C for 30 min; curve 3, 200 °C for 30 min + 250 °C for 30 min.

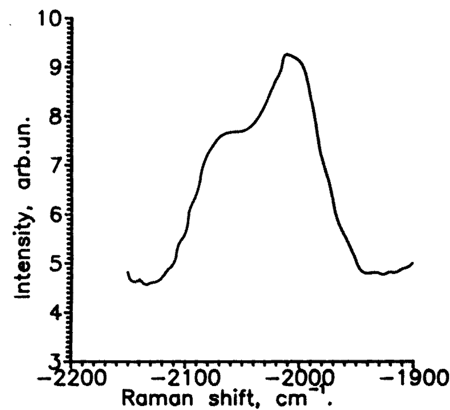

Figure 2. Raman spectrum of local hydrogen modes in the initial a-Si film.

3.2. Rapid thermal annealing

The various RTA and ELA treatments were used for stimulation of nucleation. The size of samples was about 10 mm, and no shrinkage or warping was observed after RTA and ELA. Comparison of the crystallization kinetics at 550 °C of an as-deposited a-Si film and of a sample treated by RTA (700 °C) is presented in figure 4(*b*). A typical crystallization time at 550 °C for as-deposited a-Si was determined to be about 100 h, while use of preliminary RTA reduced it to 6 h. The changes in the Raman spectra during the thermal annealing of a RTA-treated sample are shown in figure 4(*a*). Right after the RTA, one can see in the spectrum a small narrow peak at around 517 cm^{-1}, indicating the appearance of a crystal phase in an amorphous environment. After the 6 h thermal anneal the intensity of this peak was strongly increased, showing nearly 100% crystalline phase content. The symmetry of the Raman peak and its width (about 4.6 cm^{-1}) demonstrated the absence of strong phonon scattering at distances less than 500 Å.

3.3. Excimer laser annealing

Excimer laser treatments with energy density from 75 to 110 mJ cm^{-2} were used to stimulate nucleation. Figure 5 shows the Raman spectrum of sample after ELA at 110 mJ cm^{-2}. The

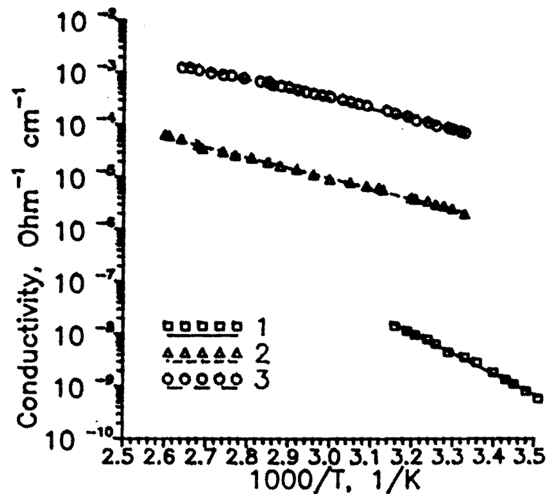

Figure 3. Conductivity of a-Si (curve 1) and poly-Si (curve 2, TA at 550 °C; curve 3, ELA + TA at 550 °C) films versus temperature.

crystal phase is clearly seen in the Raman spectrum as a small peak at 513 cm^{-1}. One can see, in the spectrum, peaks related to both crystal and amorphous parts of the specimen. After ELA treatments with an energy density above 110 mJ cm^{-2} the crystallization process occurs at a temperature below 350 °C. Figure 6 shows the evolution of the Raman peak related to the crystal phase during the process of annealing in the temperature range 200–450 °C. During the annealing the intensity of the peak has increased and its position shifted to a higher energy, which demonstrated the growth of grains. Asymmetry of the peak (i.e. a low-energy slope in the region 460–500 cm^{-1}) indicates the presence of an amorphous phase and the small-grain structure of the films.

The kinetics of crystallization during TA at *550* °C of the ELA-treated samples is shown in figure 7. On varying the energy density of ELA, one can change the incubation period of crystallization (figure 7) by forming different proportions of crystalline and amorphous phases in these films. After ELA with an energy density less than 75 mJ cm^{-2}, no difference between the crystallization kinetics of ELA-treated and as-deposited films was detected. A difference was observed in the case of ELA with an energy density of 90 mJ cm^{-2}, but the time of crystallization at 550 °C was still relatively long (about 75 h). The Raman spectra of the as-deposited a-Si film and the polycrystalline film obtained with the use of optimal ELA and TA (550 °C) treatments are shown in figure 8. As one can see, the amorphous phase is completely transformed to the crystalline phase in the treated sample. The low-energy slope disappeared. The symmetry and small width of the Raman peak at 518 cm^{-1} indicate that the concentration of grains with small sizes (less than 500 Å) is not significant.

3.4. Thermal annealing at 550 °C

Figures 9(*a*) and 9(*b*) show the electron diffraction pattern and the dark-field TEM image of a-Si film after TA (550 °C). TA at a temperature of 550 °C results in a polycrystalline structure with large grains of dendritic form. The size dispersion of grains is very broad (from 0.3 to 3.5 μm) and the orientations of neighbouring grains are different. The shapes of

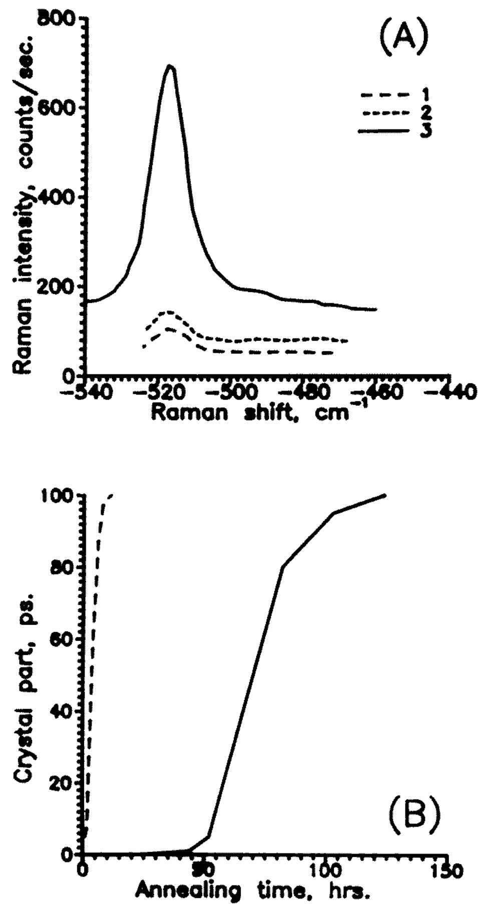

Figure 4. (A) Raman spectra of Si films after RTA (700 °C for 5 min) and TA at 550 °C: curve 1, right after RTA; curve 2, RTA + 2 h; curve 3, RTA + 6 h. (B) Kinetics of crystallization for Si films with preliminary RTA (- - - -) and without RTA (——) during the TA at 550 °C.

the grains vary from oblong to dendritic. Such polycrystalline films had a comparatively low conductivity (figure 3, curve 2), because of the high concentration of electron states on grain boundaries, which led to decreases in the mobility and conductivity. As mentioned above, low-temperature (200–500 °C) IA leads to structural changes in the amorphous phase (see figure 1). Use of IA (200–500 °C) before TA (550 °C) did not have a radical influence on the crystallization process. The grain structure remained very similar to the grain structure shown in the figure 9(*b*).

3.5. Texture and large-grain polycrystalline silicon

Using RTA (700 °C for 5 min) to stimulate nucleation led to a marked reduction in crystallization time during the subsequent TA (550 °C) from 100 to 6 h. The structure of the polycrystalline Si films was non-uniform (figure 10). In figure 10(*c*), one can see the light-field TEM image of the textured area and overprinted the corresponding electron diffraction pattern. The texture is seen to be formed by the very small crystallites with sizes

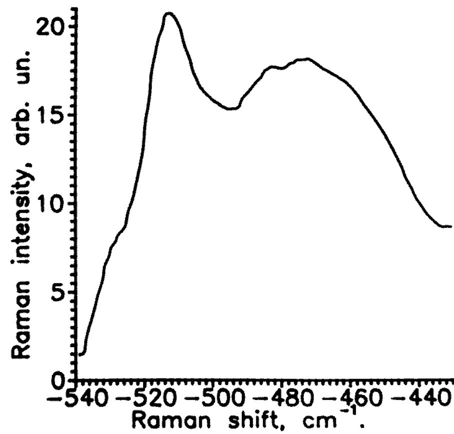

Figure 5. Raman spectrum of Si film after ELA with a low energy density.

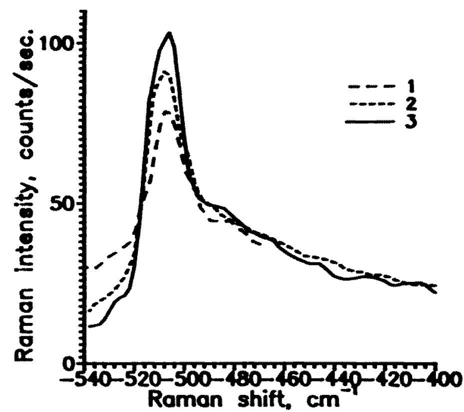

Figure 6. Raman spectra of Si films after ELA and IA: curve 1, 200 °C for 13 min; curve 2, 200–350 °C for 30 min, with steps of 50 °C; curve 3, 200–450 °C for 30 min, with steps of 50 °C.

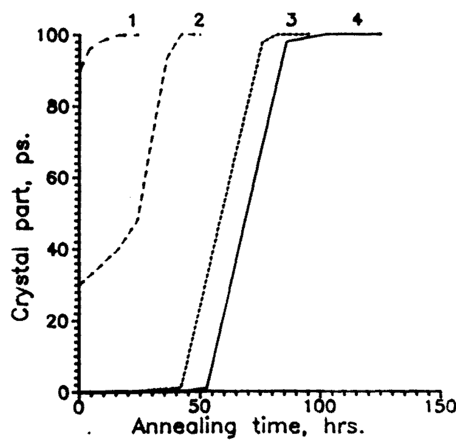

Figure 7. Kinetics of crystallization for Si films with preliminary ELA (for various energy densities: curve 1, 100% ($\equiv$ 300 mJ cm^{-2}); curve 2, 50%; curve 3, 25%) and for the initial Si film (curve 4) during TA at 550 °C.

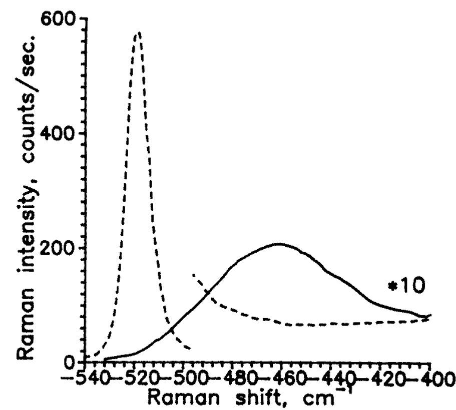

Figure 8. Raman spectra of initial a-Si film and poly-Si film after ELA and TA at 550 °C.

about several hundreds of ångströms. The crystallites with predominant orientation form the zigzag configuration. The grain sizes in the large-grain areas reach 2 μm, as one can see in figure 10(d).

Using ELA with various energy densities, one can vary the concentration of stable nuclei and, therefore, the average size of crystallites. ELA with energy densities above 110 mJ cm^{-2} creates a large number of nuclei. As a result, after subsequent TA of these films, small-grain-size polycrystalline structures were observed (with average grain size about 0.2 μm). The light-field TEM image of sample with previous ELA (90 mJ cm^{-2})

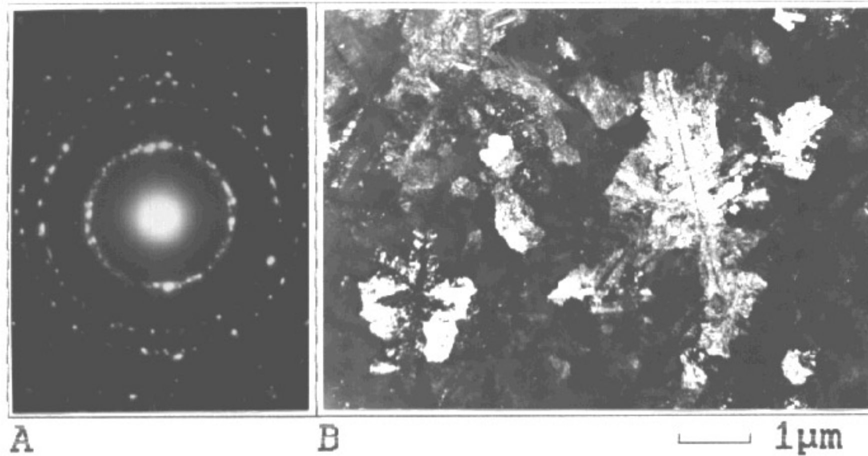

Figure 9. (*a*) Electron diffraction pattern (A) and (B) dark-field TEM image (B) of Si film after TA at 550 °C.

for stimulation of nucleation and following TA (550 °C) is shown in figure 11. As one can see, the polycrystalline film in this case is composed of crystallites of round shape and approximately equal sizes (about 2 μm). It should be noted that the grain size dispersion in this case is essentially smaller than in the case of only TA (see figure 9). The previous ELA has improved the electrical parameters of the film, which is confirmed by the data on the conductivity. The conductivity versus temperature of the films manufactured by the process of SPC during TA at 550 °C without previous ELA (curve 2) and with previous ELA (90 mJ cm^{-2}) before TA (curve 3) are shown in figure 3. Use of this stimulation of nucleation has led to an increase in the conductivity of films of up to 30 times.

A reduction in the energy density of the previous ELA down to 75 mJ cm^{-2} has led to the formation of large textured areas with sizes of 20–30 μm in the SPC process at 550 °C. In this case, the amount of non-textured areas was decreased to 20–30%. Figures 12(*a*) and 12(*b*) show the electron diffraction pattern and the light-field TEM image of the polycrystalline film manufactured in these conditions. The electron diffraction data (figure 12(*a*)) confirm that the grains have mostly similar orientations (the arcs of electron diffraction transform to separate points). In figure 12(*b*), one can see oblong single-crystal blocks growing along two $\langle 111 \rangle$ directions and one $\langle 110 \rangle$ direction; so the common orientation of these blocks is near to $\langle 110 \rangle$. The bright-field image of the non-textured large-grain area of this film is shown in figure 12(*c*). As one can see, large grains with sizes 3–3.5 μm were formed in this case.

4. Discussion

The properties of the manufactured polycrystalline films are conditioned by the processes of nucleation and crystallization. The resultant film structure is determined by competition between the growth and generation of nuclei. In order to obtain a structure with large grains, it is necessary to introduce a small concentration of nuclei and to retard spontaneous nucleation. The introduction of a definite concentration of stable nuclei and its successive growth were proposed as the main idea of this work. To realise this idea, the initial a-Si film must not contain microcrystallites. Analysis of the initial amorphous films showed

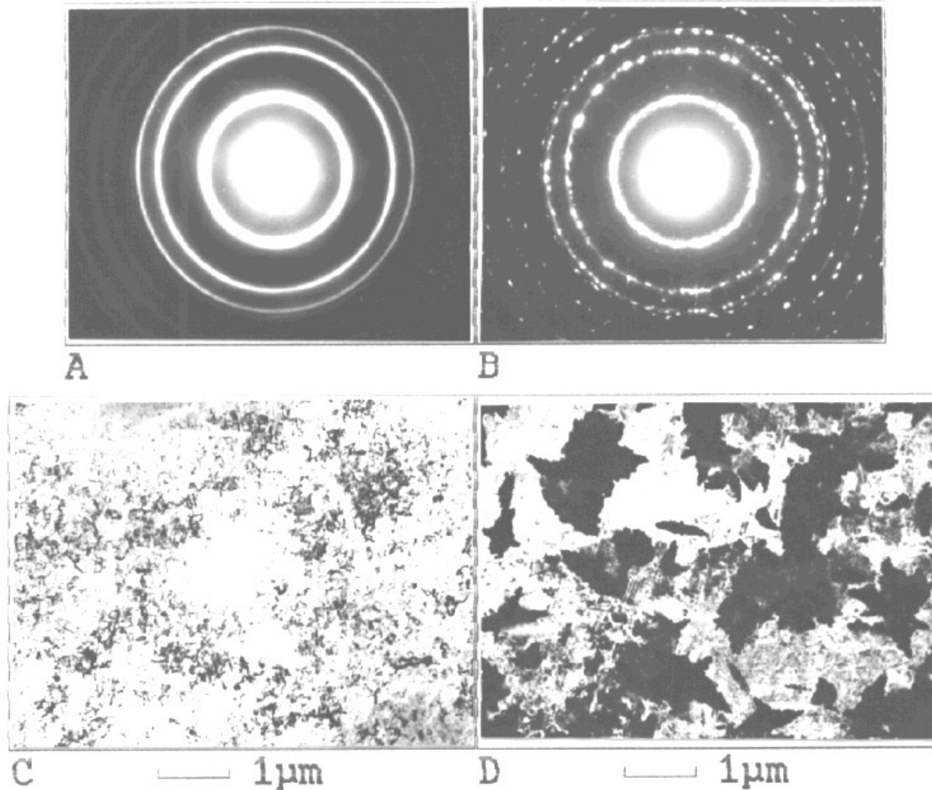

Figure 10. (A), (B) Electron diffraction patterns and (C), (D) TEM images for various areas of Si films after RTA and TA at 550 °C: (*a*) small-grain polycrystalline area, (*c*) the textured area; (*b*), (*d*) large-grain polycrystalline area.

that their properties satisfy this criterion for manufacturing high-quality poly-Si films in the crystallization process.

In the process of low-temperature annealing in the range from 200 to 350 °C an increase in the Raman scattering intensity both in amorphous and in polycrystalline films was observed (figures 1 and 6). The observed increase in a-Si (figure 1) cannot be explained as caused by hydrogen removal from the films during the annealing process. When the hydrogen is removed, the absorption coefficient increases and, consequently, the Raman scattering intensity must decrease. So this increase was probably due to structural changes in the amorphous phase. However, these changes had no marked influence on the subsequent processes of nucleation and crystallization. The increase in the Raman scattering intensity in polycrystalline films (figure 6) could be connected with the growth of crystal phase in these ELA-treated films. The crystallization rate estimated from figure 6 contradicts the established crystallization rates at 550 °C if one takes into account the values 2.6–4.4 eV for the activation energy of crystallization [29].

The successive results using RTA and ELA for stimulation of nucleation enabled us to suppose that the process of nuclei introduction must be controlled. Varying the regimes of these previous treatments, one can create a definite concentration of nuclei, reduce the incubation time and change the crystallization kinetics. The time of crystallization is

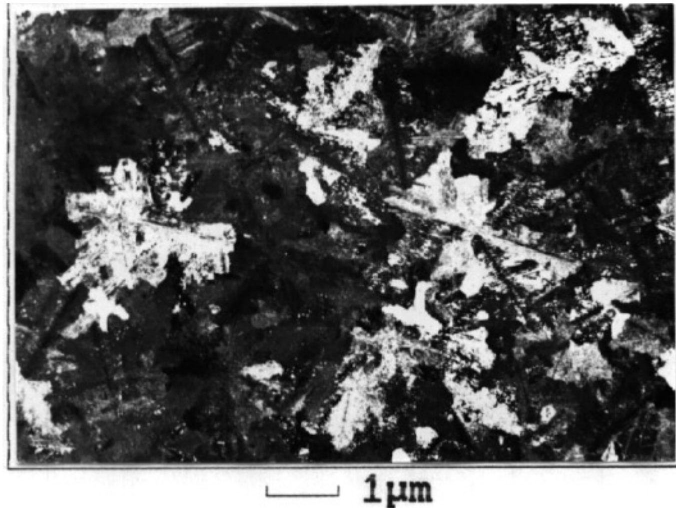

Figure 11. Bright-field TEM image of the Si film after ELA with optimal parameters and TA at 550 °C.

dependent on the concentration of the nuclei stable at the temperature of SPC. The creation of a high concentration of stable nuclei leads to a marked reduction in the incubation time (figure 7, curves 1 and 2). However, as a result of this, the manufactured films have a small-grain structure. The optimization of the regimes of ELA allows us to create homogeneous polycrystalline films with grain size 2–3 μm (figure 11).

4.1. Mechanism of polycrystalline silicon texturing

In the case of previous ELA with a beam energy density of 75–90 mJ cm^{-2}, textured films on non-oriented glass substrates were manufactured for the first time. Analysis of the electron microscopy data shows that the textured grains have a predominant (110) orientation (figure 12). It is known that the textured films were manufactured directly by the PCVD method [8, 9]. The effect of the appearance of a predominant orientation was interpreted to be the result of the different crystallization rates for different directions of crystallization. During the deposition process the vertical growth of film takes place and nuclei with an orientation corresponding to the maximal rate grow more rapidly, making this orientation predominant. So, using this interpretation, in [8] the predominance of the (110) orientation and in [9] the predominance of the (100) orientation were explained. The contradiction of [8] and [9] and the fact that the grain size is much greater than the thickness of the film (therefore, the lateral, and not the vertical, growth of grains takes place in this case) do not allow us to use this interpretation for the data obtained. The predominant orientation can be explained to be the result of the influence of mechanical stresses, both existing in the initial films and appearing due to grain formation in the amorphous matrix. The stress tensor in a thin film with a free surface has two non-zero components $\sigma_{xx} = \sigma_{yy} = \sigma$ (the z axis is perpendicular to surface) [30]. The elastic forces in the normal direction are absent. In this case, the elastic free energy of nucleus depends on its orientation. Therefore, during nucleation, the formation of nuclei with an orientation corresponding to the minimum elastic energy is more favourable and, as a result, the polycrystalline film will have the predominant orientation of the grains. The structural non-uniformities observed in the films (the presence

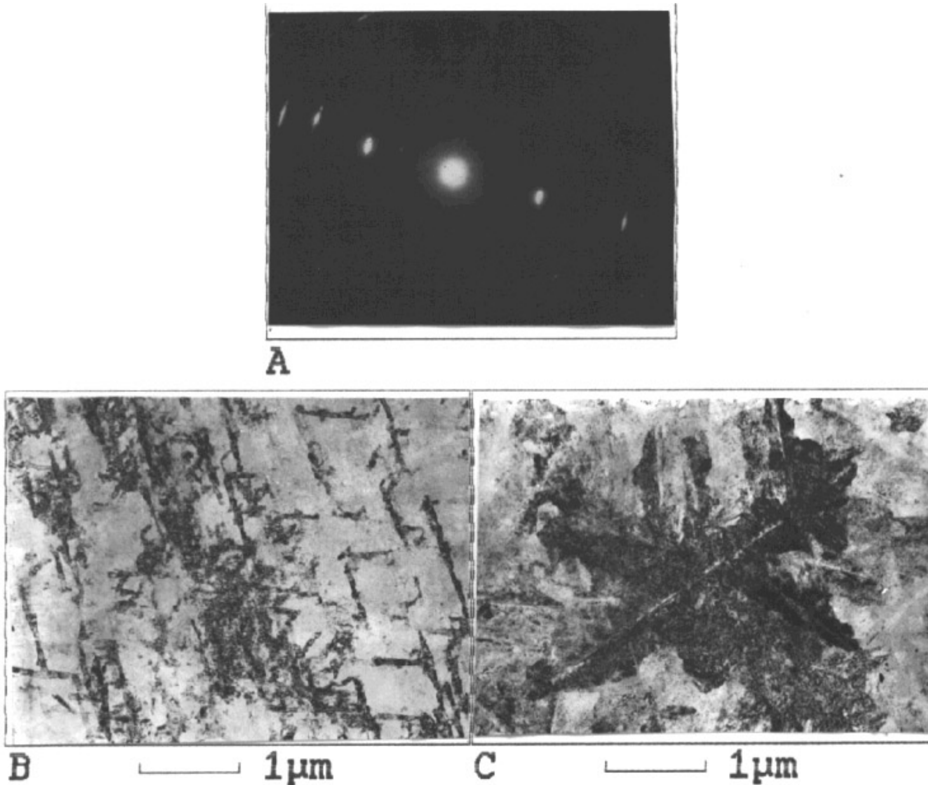

Figure 12. (*a*) Electron diffraction pattern and (*b*), (*c*) bright-field TEM images of the Si film after ELA (75 mJ cm^{-2}) and TA at 550 °C: (*a*), (*b*) textured area; (*c*) large-grain polycrystalline area.

of small-grain areas besides the textured areas) is probably caused by non-uniformity of the stresses in the structure.

4.2. The role of stresses in the kinetics

The data obtained as well as the available literature data convinced us that the mechanical stresses play a very significant role in the processes of nucleation in thin silicon films. Except for the appearance of orientation, the kinetics of nucleation can be changed in the presence of the stresses, which can be useful in explaining the different kinetics parameters observed for different silicon structures. Let us consider the influence of both external and internal mechanical stresses on the kinetics of nucleation of Si films on non-oriented substrates. The change in Gibbs thermodynamic potential in the phase transition can be written as

$$\Delta F = -\Delta\mu N + \rho_s S + \Delta F_\sigma \qquad (1)$$

where $\Delta\mu$ is the difference between the chemical potentials of poly-Si and a-Si, N is the number of atoms in the nucleus, ρ_s is the density of the surface energy, S is the area of the nucleus surface, ΔF_σ is the difference in the strain energy of film caused by formation of

the nucleus which is given by

$$\Delta F_\sigma = \int (\sigma_{ik}^0 u_{ik}^d + \tfrac{1}{2}\sigma_{ik}^d u_{ik}^d)\,\mathrm{d}V \tag{2}$$

where u_{ik}^d and σ_{ik}^d are the strain and the stress tensors, respectively, corresponding to the nucleus of the crystal phase in an amorphous film, and σ_{ik}^0 is the stress tensor in the initial film without nuclei. We neglect the influence of the mechanical stress corresponding to other nuclei on the mechanical stress around the nucleus considered. To estimate the influence of the mechanical stresses on phase transition kinetics we consider the formation of a nucleus of round shape in an a-Si film on glass. As mentioned above, the stress tensor in the initial film without nuclei has two non-zero components $\sigma_{xx} = \sigma_{yy} = \sigma$ (the z axis is perpendicular to surface). Stresses appearing due to the formation of the nucleus can be regarded approximately as stresses caused by a dilation centre of round shape in an indefinite environment. The vector of displacement for the case of spherical symmetry is $u_r = c_1 r + c_2/r^2$. Inside the nuclei this vector is $u_r = c_1 r$, and outside it is $u_r = c_2/r^2$. The strain and the stress tensors have the diagonal form with the following components: inside the nucleus,

$$u_{rr} = u_{\theta\theta} = u_{\varphi\varphi} = C_1 \qquad \sigma_{rr} = \sigma_{\theta\theta} = \sigma_{\varphi\varphi} = 3KC_1 \tag{3}$$

and, outside the nucleus,

$$\begin{gathered} u_{rr} = -2C_2/r^3 \qquad u_{\theta\theta} = u_{\varphi\varphi} = C_2/r^3 \qquad \sigma_{rr} = -4MC_2/r^3 \\ \sigma_{\theta\theta} = \sigma_{\varphi\varphi} = 2MC_2/r^3 \end{gathered} \tag{4}$$

where K and M are the modulus of dilation for c-Si and the shear modulus for a-Si, respectively.

The total change in volume due to the different densities of c-Si and a-Si is $\Delta V = V\Delta\rho/\rho$; on the other hand, $\Delta V = 4\pi r^2 u_r|_{r\gg a} = 4\pi C_2$ (a is the radius of the nucleus), which allows us to define C_2 as $C_2 = \Delta V/4\pi$. From the boundary condition (the equality of stresses on the nucleus—a-Si interface), one can calculate $C_1 = (4M/3K)(C_2/a^3) = (\Delta V/4\pi)(\gamma/a^3)$, where $\gamma = 4M/3K$. Integrating equation (2) in spherical coordinates, one can define ΔF_σ as

$$\Delta F_\sigma = \left[\frac{2\gamma\delta\rho}{3\rho}\sigma^0 + \frac{2M(\gamma+1)}{3}\left(\frac{\delta\rho}{\rho}\right)^2\right]V \tag{5}$$

where V is the volume of the nucleus given by $V = m_{at}N/\rho$. It should be noted that $\Delta F_\sigma > 0$, because the second addend in equation (5) is always positive and, although the first addend can change its sign, in this tensile stress case, $\Delta\rho/\rho = 0.03 > 0$ and $\sigma^0 > 0$. ΔF_σ is proportional to the number of atoms in the nucleus; so the influence of the mechanical stresses can be taken into account by using the effective difference in the chemical potentials:

$$\Delta\mu^* = \Delta\mu - \frac{m_{at}}{\rho}\left[\frac{2\gamma\delta\rho}{3\rho}\sigma^0 + \frac{2M(\gamma+1)}{3}\left(\frac{\delta\rho}{\rho}\right)^2\right]. \tag{6}$$

The estimation of this additional difference to $\Delta\mu^*$ gives the values 0.27 meV and 11.4 meV per atom for the first and second components, respectively, of equation (6). Hence, the influence of the mechanical stresses leads to a decrease in $\Delta\mu^*$ and an increase in the size of the critical nucleus, because

$$N_c = \frac{32\pi}{3}\rho_s^3\left(\frac{m_{at}}{\rho}\right)^2|\Delta\mu|^{-3}. \tag{7}$$

The incubation time is also increased:

$$t_{inc}(N_c) \sim N_c^{1/3} \sim |\Delta\mu|^{-1}.$$

Therefore, the appearance of mechanical stresses around the nucleus during the process of nucleation always leads to an increase in the incubation time. The analysis of equation (6) shows that the influence of the residual stresses in the film on the process of nucleation corresponds to the Le Chatelier–Braun principle. The nucleation rate increases in the case of a stress decrease due to nucleus formation and decreases when the stress increases. Using this interpretation, one can analyse the appearance of the predominant orientation of grains, taking into account the dependence of the stress tensor around the nucleus on its orientation, which probably will allow us to explain the predominance of the (110) orientation for grains in poly-Si films on glass.

5. Conclusions

It has been shown that the use of RTA and ELA for stimulation of nucleation made it possible to manufacture homogeneous poly-Si films on glass with grain sizes up to 3 μm at temperatures below 550 °C. The use of the RTA enables us to reduce considerably the incubation time (from 100 to 6 h). Textured silicon films on glass with predominant (110) orientation and sizes of textured areas up to 30 μm were manufactured using excimer laser stimulation of nucleation. The influence of the mechanical stress mechanism on grain orientation was suggested and the main aspects of this mechanical stress influence on the kinetics of nucleation were theoretically considered in terms of the classical theory of nucleation. We obtained the result that the mechanical stresses appearing due to grain growth in the amorphous matrix leads to an increase in incubation time.

Acknowledgments

The authors would like to thank Professor I G Neizvestny for a significant contribution to this work, for useful discussion and for comments, and Dr S A Kochubei for helping with the excimer laser treatments.

References

[1] Shi G and Seinfeld J H 1991 *J. Mater. Res.* **6** 2091
[2] Kashchiev D 1969 *Surf. Sci.* **14** 209
[3] Oxtoby D W 1992 *J. Phys.: Condens. Matter* **4** 7627
[4] Oxtoby D W 1992 *Fundamentals of Inhomogeneous Fluids* ed D Henderson (New York: Marcel Dekker) p 407
[5] Stiffler S R, Evans P V and Greer A L 1992 *Acta Metall. Mater.* **40** 1617
[6] Spaepen F and Turnbull D 1982 *Laser Annealing of Semiconductors* ed J M Poate and J W Mayer (New York: Academic) p 15
[7] Meakin D B, Coxon P A, Migliorato P, Stoemenos J and Economou N A 1987 *Appl. Phys. Lett.* **50** 1894
[8] Kakinuma H, Mohri M, Sakamoto M and Tsuruoka T 1991 *J. Appl. Phys.* **70** 7374
[9] Nagahara T, Fujimoto K, Kohno N, Koshiwagi Y and Kakinoki H 1992 *Japan. J. Appl. Phys.* **31** 4555
[10] Czubatyj W, Beglau D, Chao B S, Gonzales-Hemandez J, Pawlik D A, Clersy P, Jablonski D and Himmler R 1991 *J. Vac. Sci. Technol.* A **9** 294
[11] Czubatyj W, Beglau D, Himmler R, Jablonski D and Guha S 1989 *IEEE Electron Devices Lett.* **10** 349
[12] Kakkad R, Liu G and Fonash S J 1989 *J. Non-Cryst. Solids* **115** 66
[13] Liu G and Fonash S J 1989 *Appl. Phys. Lett.* **55** 660
[14] Sameshima T and Usui S 1991 *J. Appl. Phys.* **70** 1281

[15] Kuriyama H, Kuwahara T, Ishida S, Nohda T, Sano K, Iwata H, Noguchi S and Kuwano S 1992 *Japan. J. Appl. Phys.* **31** 4550

[16] Choi D-H, Shimizu K, Sugiura O and Matusmura M 1992 *Japan. J. Appl. Phys.* **31** 4545

[17] Miyata Y, Furuta M, Yoshioka T and Kawamura T 1992 *Japan. J. Appl. Phys.* **31** 4559

[18] Kuriyama H, Kiyama S, Noguchi S, Kuwahara T, Ishida S, Nohda T, Sano K, Iwata H, Kawata H, Osumi M, Tsuda S, Nakano S and Kuwano Y 1991 *Japan. J. Appl. Phys.* **30** 3700

[19] Bolotov V V, Efremov M D, Volodin V A, Lipatnikov E A, Fedina L I and Neizvestnij I G 19– *Technical Report of the Institute of Semiconductor Physics* sent to Samsung Advanced Institute of Technology October 1992

[20] Bolotov V V, Efremov M D, Fedina L I, Lipatnikov E A, Volodin V A and Neizvestnij I G 1993 *Abstracts Spring Meet. Materials Research Society-93 (San Francisco, CA, 1993)* p A9.54

[21] Beeman D, Tsu R and Thorpe M F 1985 *Phys. Rev.* B **32** 874

[22] Alben R, Weaire D, Smith J E Jr and Brodsky M H 1975 *Phys. Rev.* B **11** 2271

[23] Hishikawa Y 1987 *J. Appl. Phys.* **62** 3150

[24] Kanelis G, Morhange J F and Balkanski M 1980 *Phys. Rev.* B **21** 1543

[25] Cheng G-X, Xia H, Chen K-J, Zhang W and Zhang X-K 1990 *Phys. Status Solidi* a **118** K51

[26] Tsu R, Gonzales-Hernandes J, Chao S S, Lee S C and Tanaka K 1982 *Appl. Phys. Lett.* **40** 534

[27] Okada T, Iwaki T, Kasahara H and Yamamoto K 1985 *Japan. J. Appl. Phys.* **24** 161

[28] Bustarret E, Hachicha M A and Brunel M 1988 *Appl. Phys. Lett.* **52** 1675

[29] Suzuki M, Hiramoto M, Oguiura M, Kamisaka W and Hasegawa S 1988 *Japan. J. Appl. Phys.* **27** L1380

[30] Bolotov V V, Efremov M D and Volodin V A 1994 *Thin Solid Films* **248** 212